Associations between timing and magnitude of spring blooms and zooplankton dynamics in the southwestern Barents Sea

Running title: Spring blooms and zooplankton dynamics

Kaixing Dong[1,*], Kristina Øie Kvile[1, 2], Nils Chr. Stenseth[1], Leif Chr. Stige[1, 3]

[1]Centre for Ecological and Evolutionary Synthesis (CEES), Department of Biosciences, University of Oslo, PO Box 1066 Blindern, 0316 Oslo, Norway

[2]Norwegian Institute for Water Research, Gaustadalléen 21, 0349 Oslo, Norway

[3]Norwegian Veterinary Institute, PO Box 750 Sentrum, 0106 Oslo, Norway

***Corresponding author: kaixingd@mail.uio.no**

ABSTRACT

During the past decades many high-latitude marine systems have experienced a strong warming trend with yet poorly understood consequences for trophic coupling and ecosystem functioning. A key knowledge gap is how timing and magnitude of phytoplankton blooms influence higher trophic levels. In this study, we investigated associations between timing and magnitude of phytoplankton blooms and dynamics of three size fractions of mesozooplankton from 1998 to 2019. The study focused on the southwestern Barents Sea, an Arctic shelf sea area that is dominated by relatively warm Atlantic waters and remains ice-free year-round. Results showed that an early spring bloom (late April - early May) was associated with high biomass of medium-sized (1–2 mm) zooplankton in areas "down-stream" of the phytoplankton bloom along with the prevailing currents. Conversely, a late spring bloomwas associated with high biomass of small-sized (0.180–1 mm) zooplankton, with no spatial shift. High peak magnitude of the bloom (>5 mg chlorophyll *a* m^{-3}) was associated with low zooplankton biomass, suggesting either top-down control or that the zooplankton utilized intense and presumably short blooms inefficiently. For small- and large-sized (>2 mm) zooplankton, the relationship was nonlinear, as zooplankton biomass was also low when bloom peak magnitude was very low (<4 mg chlorophyll *a* m^{-3}). Our findings imply that if phytoplankton blooms in the region become earlier, this will increase the biomass of medium-sized zooplankton that are important prey for planktivorous fishes. Moreover, our study highlights that increased biomass of phytoplankton does not necessarily translate into increased zooplankton biomass.

KEY WORDS: Southwestern Barents Sea · phytoplankton blooms · zooplankton biomass · generalized additive models · trophic coupling

1. INTRODUCTION

Phytoplankton are the main primary producers of marine food webs, and pelagic and benthic secondary production and biogeochemical cycles rely in large part on the activities of these microscopic organisms (Nixon et al. 2009, Behrenfeld & Boss 2014, Griffiths et al. 2017). The seasonal cycle of phytoplankton at high latitudes is characterized by short but intense spring blooms with high biomass in surface layers, sometimes followed by a second bloom in autumn. The timing and magnitude of phytoplankton blooms are influenced by a wide range of abiotic and biotic factors, including availability of nutrients and light, water temperature, salinity, stratification and mixing, as well as grazing pressure from zooplankton (Ueyama & Monger 2005, Sommer et al. 2012, Cloern et al. 2014). The seasonal cycles of zooplankton and other organisms in high-latitude food webs are timed to utilize the short boosts in productivity. Understanding how variability in timing and magnitude of phytoplankton blooms influence higher trophic levels is important to understand the functioning of marine food webs.

Climate change influences many of the physical factors that control pelagic phytoplankton blooms (Guinder & Molinero 2013), which may lead to shifts in the timing, composition and magnitude of the blooms (Wassmann 2011, Kahru et al. 2016, Dong et al. 2020), and the transfer of energy to higher trophic levels (Richardson 2008, Reygondeau & Beaugrand 2011, Winder & Sommer 2012). Warmer temperatures have been associated with decreased phytoplankton peak biomass, reduced mean cell size, decreased proportion of diatoms in the phytoplankton biomass (Sommer & Lengfellner 2008) and earlier bloom timing (Lewandowska & Sommer 2010). These changes might result in less advantageous feeding conditions for major copepod zooplankton species and, thus, in a less efficient energy transfer from primary producers to higher trophic levels under a warmer climate. Simultaneously, climate

change influences the size distribution of the zooplankton community, both through intra-specific changes in body size and through shifts in species composition, often leading to increased dominance of smaller-sized zooplankton (Rice et al. 2015, Møller & Nielsen 2020). This size shift will influence predators that prefer a certain prey size (Blanchard et al. 2017) and thus the energy transfer to higher trophic levels. Therefore, it is relevant to investigate environmental effects on zooplankton of different size classes.

Changes in the timing and magnitude of phytoplankton blooms influence the zooplankton that feed on them. A long-term study (1994–2009) on the southeastern Bering Sea shelf indicated that the magnitude and timing of phytoplankton blooms was significantly associated with interannual changes in copepod composition (Ohashi et al. 2013). On the US Northeast Continental Shelf, different regions show different relationships between zooplankton biovolume and spring bloom biomass and timing. Specifically, on the Georges Bank, spring zooplankton biovolume was positively correlated with average chlorophyll concentrations during the bloom period. However, in the western Gulf of Maine, biovolume was instead positively correlated with the spring bloom start timing and negatively correlated with peak magnitude of the bloom (Friedland et al. 2015). In the northeastern Norwegian Sea and southwestern Barents Sea, a combination of shallow mixed layer depth and high wind speed in spring was linked to increased chlorophyll biomass in spring and increased *Calanus finmarchicus* biomass in summer, suggesting that increased spring bloom magnitude or duration positively influenced the population growth of this copepod (Kvile et al. 2016).

Ocean currents play important role in the interaction between phytoplankton and zooplankton. In some systems that are highly advective, seasonal changes in flow pattern have a strong association with observed changes in zooplankton abundance and composition (Hooff &

Peterson 2006). Accounting for advection is, however, a challenge in statistical analyses of associations between phytoplankton bloom phenology and zooplankton dynamics. Such analyses have to take into account that zooplankton are likely to be influenced by phytoplankton earlier in the year at a different geographic location than where the zooplankton were sampled.

We here focus on the southwestern Barents Sea (Fig. 1). The Barents Sea is a productive Arctic shelf sea located to the north of Norway and northwestern Russia. As a transition zone between the Arctic Ocean and the North Atlantic, the Barents Sea is influenced by three major currents: The Norwegian Atlantic Current flows northeastwards along the Atlantic coast of Norway and turns eastwards into the Barents Sea; the Norwegian Coastal Current follows the coast from the southwest and turns eastwards in the Barents Sea as the North Cape current; The Arctic Current comes from the north-northeast and dominates the northern Barents Sea (Mosby 1968, Ersdal 2001, Ingvaldsen et al. 2004, Asplin et al. 2006). The southwestern Barents Sea is influenced by relatively warm Atlantic and Coastal water masses, and is ice-free year-round. The mesozooplankton community here is dominated by the copepod *C. finmarchicus* (Aarflot et al. 2018), which is transported into the Barents sea with the prevailing currents from the distribution center in the Norwegian Sea (Edvardsen et al. 2003, Aarflot et al. 2018). *C. finmarchicus* typically constitutes more than 75% of the mesozooplankton biomass in our study region, but the contribution of *C. finmarchicus* varies interannually from 40% to close to 100% (Aarflot et al. 2018).

The aim of this study was to reveal the associations between the timing and magnitude of phytoplankton blooms and zooplankton dynamics in the southwestern Barents Sea. Our work focuses on: 1) how phytoplankton phenology affects the dynamics of different zooplankton size

classes, and 2) at which spatial scales the phytoplankton bloom timing and magnitude have significant impacts on zooplankton biomass in this advective environment.

2. MATERIALS & METHODS

2.1 Study area

Our study was carried out in the southwestern Barents Sea between 71° and 75° N and 17.5° and 33.5° E. We divided this research region into four parts, which we refer to as sections A-D (Fig. 1). Each section covered 4 degrees of longitude. Section A is westernmost and "upstream" in the prevailing currents and D is easternmost and "downstream". The southern limit was 71° N for all sections while the northern limit was 74° N for sections A and B, 74.5° N for section C and 75° N for section D. These northern limits were decided to restrict the study area to Atlantic-dominated waters, here defined as areas where long-term average temperatures are >3°C, using mean temperature at 100 m depth during zooplankton surveys in August-early October 1981–2010 as reference (Stige et al. 2014).

2.2. Data

2.2.1 Data description

Zooplankton data were collected from 1998 to 2019 by the Institute of Marine Research, Norway (Fig. 2). Most data are from August-September, and we also have data from January-March, and from June before 2006 (supplementary Fig. S1). There were no trends over time in the distribution of sampling effort with latitude (Fig. S1).

Samples were collected by vertically towed WP2 plankton nets (56 cm opening diameter, 180 µm mesh size) from near the bottom to the surface. The biomass samples were sieved successively through three meshes: 2 mm, 1 mm and 180 µm, providing biomass estimates for the >2 mm (large-sized), 1–2 mm (medium-sized) and <1 mm (small-sized) size

fractions (Dalpadado et al. 2020). Typical organisms in the small-sized fraction were eggs, nauplii and copepodite stages CI-III of *C. finmarchicus* and small copepods such as *Oithona* spp., typical medium-sized organisms were CIII-VI of *C. finmarchicus* and typical large-sized organisms were krill, amphipods and large copepods such as *Calanus hyperboreus* (Gjøsæter et al. 2002). It is noteworthy that both the smallest and the largest zooplankton were probably under-sampled, as the small zooplankton might slip through the mesh and the large ones may escape the net by swimming. Only zooplankton data from section D was used for our study (N = 567 samples, Figs. 1 and 2).

We used satellite derived chlorophyll *a* (Chl-*a*) data covering March−September 1998−2019 as proxy of phytoplankton biomass (Fig. 3). We extracted merged level-3 case I ocean Chl-*a* concentration data (mg m^{-3}) from the GlobColour database (http://hermes.acri.fr) with a spatial resolution of 0.25° latitude × 0.25° longitude and a temporal resolution of 8 days. The Chl-*a* data were created with a Garver-Siegel-Maritorena (GSM) model (Maritorena et al. 2010) and merged the normalized water-leaving radiance observations from several ocean color sensors for better coverage: sea-viewing Wide Field-of-view Sensor (Sea-WiFS), MEdium Resolution Imaging Spectrometer (MERIS), Moderate Resolution Imaging Spectroradiometer (MODIS) and Visible Infrared Imaging Radiometer Suite (VIIRS). These satellites collect visible and near-infrared solar radiation reflected from the ocean surface layer. It should be noted that the remotely sensed information is only available during the daytime with adequate light and in the absence of ice and clouds. We used Chl-*a* data from all four sections A-D (Fig. 3).

We used sea surface temperature (SST) estimates (°C) from the Advanced Very High Resolution Radiometer (AVHRR) satellite data set (NOAA OISST V2) (Reynolds et al. 2007)

with a spatial resolution of 0.25° latitude × 0.25° longitude and a temporal resolution of one day (www.esrl.noaa.gov/psd/).

2.2.2 Data processing

To match with the phytoplankton bloom dynamics, we converted the temporal scale of the zooplankton data from calendar year (January to December) to a biological year (April to March of next year). Generally, based on satellite Chl-*a* data, phytoplankton start to bloom from the end of March and the primary production season terminates in September in the southwestern Barents Sea (Signorini & McClain 2009). Consequently, the zooplankton sampled at the beginning of a year (from January to March) are potentially influenced by primary production of the previous calendar year (but current biological year). We chose peak magnitude (*pmag* = maximum Chl-*a*, [mg m^{-3}]) and peak timing (*ptime* = day-of-year of maximum Chl-*a*) of the phytoplankton bloom as indices to analyze the associations between phytoplankton and zooplankton dynamics. Specifically, we calculated *pmag* and *ptime* based on eight-day averaged Chl-*a* for each zooplankton sample location (± 0.5 degree latitude and ± 2 degree longitude) and biological year. This simple approach to identify the peak time and peak magnitude of the bloom appeared to capture the signal in the data quite well (see supplementary Fig. S2). We also estimated *pmag* and *ptime* for upstream locations of the zooplankton samples (section D), by calculating *pmag* and *ptime* at corresponding latitudes in sections A-C. As corresponding latitudes, we considered latitudes at the same fraction of the range from south to north along each section. For example, the middle latitude of section D (73º N) was considered to correspond to the middle latitudes of the other sections (i.e., 72.75º N for section C and 72. 5º N for sections A and B). This choice was based on the fact that the Atlantic and Coastal Currents generally flow

from west to east but also spread over a longer latitudinal range in the eastern part of our study area (Fig. 1).

For each zooplankton data point, we extracted the nearest SST value for the same date from the NOAA OISST V2 data set.

2.2.3 Descriptive statistics

To show interannual trends in Chl-*a* peak time and peak magnitude, we calculated annual mean values of *pmag* and *ptime* along each transect and reported the interannual mean and standard deviation (s.d.) of these values. Associations between annual averaged peak time and averaged peak magnitude of Chl-*a* were quantified by calculating the Pearson correlation coefficient. To account for autocorrelation in the time series, the effective number of degrees of freedom in the significance test for the correlation was adjusted according to the method described by Quenouille (1952) and modified by Pyper & Peterman (1998).

2.3 Statistical Modelling

2.3.1 Models considered

Generalized additive models (GAMs) (Hastie & Tibshirani 1990) were used to analyze the associations between zooplankton of section D and Chl-*a* indices from all four sections. All analyses were performed using the "mgcv" library (version 1.8-31) in R v.3.6.2 (R Core Team 2018).

The response variable was observational data on zooplankton biomass, and the explanatory variables included day-of-year of the sample, sampling depth, sea surface temperature (SST) and Chl-*a* indices (*pmag* and *ptime*) at corresponding latitudes of the sampled zooplankton in different sections. SST was included because we wanted to control for potential confounding effects of temperature and water mass distribution, which might mask associations

between Chl-*a* and zooplankton biomass. Initial models also considered latitude as predictor variable, but preliminary results showed that the spatial pattern was best explained as function of sampling depth alone.

We considered models with different levels of complexity. The simplest model explained biomass of zooplankton as function of day-of-year and sampling depth:

$$logzoo_{i,t} = f(doy_t) + g(logdepth_j) + \varepsilon_{i,t} \quad (1)$$

Here, $logzoo_{i,t}$ is the natural logarithm of the zooplankton biomass (added 1 to avoid taking the logarithm of zero) of a given size group at location *i* and time *t*; $f(doy_t)$ is a one-dimensional smooth function of day-of-year of the sample (cyclic cubic regression spline with maximum 5 knots, i.e. 4 degrees of freedom); $g(logdepth_j)$ is a one-dimensional smooth function of the natural logarithm of the sampling depth at the sample location (cubic regression spline with maximum 3 knots); and $\varepsilon_{i,t}$ is a normally distributed noise term. The number of knots were restricted to avoid overfitting and provide biologically interpretable results.

A second model also included the biological year to investigate the interannual variation in zooplankton biomass:

$$logzoo_{i,t} = f(doy_t) + g(logdepth_j) + h(year_y) + \varepsilon_{i,t} \quad (2)$$

Here, $h(year_y)$ is a one-dimensional smooth function of the biological year of the sample (cubic regression spline with 9 knots).

To explore the association between temperature and zooplankton biomass, we fitted the following model based on model 1:

$$logzoo_{i,t} = F(doy, SST) + g(logdepth) + \varepsilon_{i,t} \quad (3)$$

Here, F(*doy, SST*) is a two-dimensional tensor-product smooth function of the day-of-year and SST of the sample (with maximum 5 knots for each cubic regression spline basis function). This function shows how the seasonal development of zooplankton depends on SST.

We also investigated if the variations in zooplankton biomass could be explained by chlorophyll phenology, by adding Chl-*a* indices to Eq. 3 to investigate the unique effects of both Chl-*a* and SST. We added Chl-*a* indices into the model step by step, first investigating the association of zooplankton biomass with *ptime*:

$$logzoo_{i,t} = F(doy, SST) + g(logdepth_j) + k(ptime_{i,t}) + \varepsilon_{i,t} \quad (4)$$

Here, $k(ptime_{i,t})$ is a one-dimensional smooth function of the peak time of Chl-*a* in biological year *t* and a latitude that corresponded to the zooplankton sampling location *i* (cubic regression spline with maximum 5 knots). The Chl-*a* indices referred either to same section as the zooplankton or to one of the sections farther west (see 2.3.2 Model selection). The model assumed that a given change in *ptime* was associated with the same proportional change in zooplankton biomass throughout the biological year. We then investigated the association of zooplankton biomass with *pmag*:

$$logzoo_{i,t} = F(doy, SST) + g(logdepth_j) + l(pmag_{it}) + \varepsilon_{i,t} \quad (5)$$

Here, $l(pmag_{i,t})$ is a one-dimensional smooth function of the peak magnitude of Chl-*a* (cubic regression spline with maximum 5 knots).

In the next model, smooth effects of *ptime* and *pmag* were included additively:

$$logzoo_{i,t} = F(doy, SST) + g(logdepth_j) + k(ptime_{it}) + l(pmag_{it}) + \varepsilon_{i,t} \quad (6)$$

Further, we proceeded with varying-coefficient models (Hastie & Tibshirani 1993) that allowed the effects of *ptime* or *pmag* on zooplankton biomass to vary smoothly as a function of

day-of-year. These models investigated if the seasonal pattern in zooplankton biomass differed between years with early or late *ptime* (Eq. 7) or high or low *pmag* (Eq. 8):

$$logzoo_{i,t} = F(doy, SST) + g(logdepth_j) + K(ptime_{it,}\, doy_t) + \varepsilon_{i,t} \quad (7)$$

Here, $K(ptime_{i,t}, doy_t)$ is a one-dimensional smooth function of day-of-year that gives the coefficient for the effect of *ptime* (cubic regression spline with maximum 5 knots). Specifically, the effect of *ptime* on *logzoo* was assumed to be linear at any given day-of-year, but the coefficient for this effect varied smoothly with day-of-year.

$$logzoo_{i,t} = F(doy, SST) + g(logdepth_j) + L(pmag_{it,}\, doy_t) + \varepsilon_{i,t} \quad (8)$$

Here, $L(pmag_{i,t}, doy_t)$ is a one-dimensional smooth function of day-of-year that gives the coefficient for the effect of *pmag* (cubic regression spline with maximum 5 knots).

2.3.2 Model selection

To identify which section's Chl-*a* indices provided the best fit to the zooplankton data in section D, we considered four alternative models based on Eq. 6 for each zooplankton size group. The models differed in that Chl-*a* indices from each of the four different sections were used as predictors. The different models were compared based on the generalized cross validation value (GCV). The GCV of a model is a proxy for the model's out-of-sample predictive mean squared error. Consequently, a model with lower GCV had more predictive power and was hence preferred.

After finding which section provided the best Chl-*a* indices for each zooplankton size group, we fitted the models from Eq. 3 to Eq. 7. These models were compared to find the model formulation with the highest explanatory power for each size group. The GCV is based on an assumption that all the data are independent. As we expected that data could be correlated within years, the GCV might select overly complex models. We therefore calculated leave-one-year-out

cross validation (CV) to compare alternative model formulations with different numbers of predictor variables. We then considered year as the sampling unit. Specifically, the CV procedure was:

(i) Build a truncated data set by removing one "test" year data out.

(ii) Make out-of-sample predictions for the "test" year by refitting the models based on the truncated data set.

(iii) Repeat i-ii for all years (one year left out at a time), and

(iv) Calculate the mean squared prediction error across all years.

Since the CV increases with high complexity and low predictive power, models with lower CV are better.

3. RESULTS

3.1 Variation in phytoplankton biomass with season and year

The Chl-*a* peak time tended to occur earlier when going from west to east across the four sections (Fig. 3A-D): Section A (mean day-of-year 170.9 ± s.d. 30.6) > Section B (mean day-of-year 148.9 ± 23.5) > Section C (mean day-of-year 141.7 ± 20.6) ≈ Section D (mean day-of-year 142.0 ± 19.8). The phytoplankton peak magnitude increased when going from west to east: Section A (mean Chl-*a* 2.5 ± s.d. 0.8 mg m^{-3}) < Section B (mean Chl-*a* 3.6 ± 1.5 mg m^{-3}) < Section C (mean Chl-*a* 4.5 ± 1.7 mg m^{-3}) < Section D (mean Chl-*a* 5.6 ± 2.7 mg m^{-3}).

The peak time and peak magnitude of Chl-*a* for each section varied from year to year (Fig. 3E-L), and were negatively correlated for all sections (Pearson correlation coefficient between -0.46 and -0.60, $P < 0.05$).

3. 2 Variation in zooplankton biomass with season, sampling depth and year

Using spatiotemporal statistical analysis (Eq. 2), we separated the recurring seasonal pattern from the interannual trend and the effect of sampling depth for each zooplankton size fraction. We found strong seasonal patterns in biomasses of small- and medium-sized zooplankton, with increasing biomass from early spring to mid-summer and decreasing biomass after mid-summer (Fig. 4A and 4B). These peaks were approximately two months later than the Chl-*a* peak at section D. For the large-sized zooplankton, biomass increased slightly from spring to early autumn (Fig. 4C). Note that data gaps make the exact timing of the peaks uncertain. Biomasses of all zooplankton size groups were positively related to the sampling depth (Fig. 4D, 4E and 4F). Both small- and medium-sized zooplankton biomass varied from year to year (Fig. 4G and 4H), with peaks around years 1999, 2009 and 2017 for small-sized zooplankton and around years 2000, 2006-2011 and 2018 for medium-sized zooplankton. A negative trend was found for large-sized zooplankton biomass from 1998 to 2015, followed by an increase thereafter (Fig. 4I).

3.3 Associations between zooplankton biomass and temperature

We found significant associations between temperature and zooplankton biomass for all three size groups (Fig. 5A-C). For example, the highest biomass peak of small-sized zooplankton occurred around June at temperatures between 5 and 7 °C. A lower seasonal biomass peak occurred at temperatures higher or lower than this temperature range. For medium-sized zooplankton, we found clearest association between SST and biomass in June, when biomass was highest at relatively warm temperatures. For large-sized zooplankton, biomass in January-March as well as in August-September was highest at relatively cold temperatures.

3.4 Model selection results

We found that small-sized zooplankton were most closely associated (low GCV and high R^2 in Table 1) with local Chl-*a* indices (i.e., from section D). Medium-sized zooplankton were most closely associated with Chl-*a* indices from one section upstream (section C, Table 1). Large-sized zooplankton were most closely associated with Chl-*a* indices from three sections upstream (section A, Table 1).

Using Chl-*a* indices from the sections identified in Table 1, we conducted a new round of model selection, to compare alternative model formulations. For both small- and medium-sized zooplankton, we found that Model 6 (Eq. 6 in Table 2) with additive effects of *ptime* and *pmag* as predictor variables, performed best among the candidate models. For the large-sized zooplankton, the model with an additive effect of *pmag* and no effect of *ptime* had lowest CV value (Eq. 5 in Table 2). For all zooplankton size fractions, models with both Chl-*a* indices and SST performed better than models with only SST.

3.5 Associations between zooplankton biomass and Chl-*a* indices

The selected model for small-sized zooplankton in section D (Eq. 6 in Table 2) showed a significant association between zooplankton biomass and Chl-*a* peak time at the same section (Fig. 6A): biomass of small-sized zooplankton was lower when Chl-*a* peak time was early (e.g. April or early May) than when Chl-*a* peak time was late (e.g. late May or later). We found a significantly negative association between medium-sized zooplankton in section D and Chl-*a* peak time of section C (Fig. 6B). For large-sized zooplankton, there was no significant association between biomass and Chl-*a* peak time (hence this association is not shown in Fig. 6).

The biomass of small-sized zooplankton showed a non-linear association with Chl-*a* peak magnitude at the same section (Fig. 6D). Specifically, the zooplankton biomass increased with

increasing Chl-*a* peak magnitude up to approximately 5 mg m^{-3}. Afterwards, there was a downward trend of biomass as Chl-*a* peak magnitude increased from approximately 5 to 15 mg m^{-3}. Above a peak magnitude of 15 mg m^{-3}, the uncertainty is high because of few observations. There was a significantly negative linear association between Chl-*a* peak magnitude in section C and medium-sized zooplankton biomass in section D (Fig. 6E). Large-sized zooplankton biomass increased with increasing Chl-*a* peak magnitude of section A up to approximately 4 mg m^{-3} (Fig. 6F).

4. DISCUSSION

Our results show statistical associations between phytoplankton spring bloom timing and magnitude and zooplankton dynamics in a productive region with highly valuable fisheries. Results have implications for our understanding of how changes in phytoplankton spring bloom timing and magnitude may impact food web dynamics, as phytoplankton bloom characteristics play an important role in energy transfer to higher trophic levels (Winder & Sommer 2012).

4.1 Spatial scales of interactions

Due to the advection of Atlantic water in the southern Barents Sea, phytoplankton phenology and zooplankton development in upstream regions can be expected to influence zooplankton biomass in downstream regions. Stige et al. (2014) showed associations between zooplankton dynamics in the southwestern Barents Sea and upstream areas near the entrance to the Barents Sea the preceding summer. In our study, we found that small-sized zooplankton biomass is mainly influenced by timing and magnitude of local phytoplankton blooms while medium- and large-sized zooplankton are more strongly linked to phytoplankton phenology one and three sections upstream, respectively. This result suggests that the spatial scales of the interactions differ between zooplankton size groups, likely reflecting the different temporal

scales of their dynamics. If bloom timing and magnitude affect zooplankton reproduction (Melle & Skjoldal 1998, Hirche & Kosobokova 2003, Søreide et al. 2010), we may expect a longer temporal delay and spatial shift in the association with biomass of large than small zooplankton, simply because it takes longer time to grow into the large size fraction than the small. Hence, small zooplankton may track more closely the fluctuations in their resources. This finding further underlines that advection of water masses plays an important role in influencing the interaction between phytoplankton and zooplankton in the southwestern Barents Sea and should be accounted for in statistical analyses.

4.2 Variations in timing and magnitude of phytoplankton and zooplankton

In the Arctic Ocean, as one moves towards higher latitudes, the timing of the phytoplankton bloom tends to occur later, the amplitude of the primary production becomes lower and the duration shorter as a result of the seasonal variations in light and sea ice conditions (Falk-Petersen et al. 2007, Leu et al. 2011). How the timing of the phytoplankton bloom varies along longitudinal gradients has seldom been examined (but see Friedland et al. 2018). Our result shows that in our study area (the southwestern Barents Sea), as one moves eastward along with the Atlantic Current, the phytoplankton bloom tends to occur earlier (Fig. 3A-D), which is in line with observations from a recent study (Dalpadado et al. 2020). Generally, in the southwestern Barents Sea, phytoplankton start to bloom when stratification is slowly established by solar heating (Loeng 1991, Falk-Petersen et al. 2000, Reigstad et al. 2002, Wassmann et al. 2006). Given that all four sections are at nearly the same latitudes and in the ice-free part of the Barents Sea, we hypothesize that this timing gradient of phytoplankton blooms is caused by earlier stratification in eastern than western areas, possibly caused by lower flow velocity or weaker winds. We note that because of this longitudinal gradient in phytoplankton timing, zooplankton

that drift with the water masses from the Norwegian Sea into the Barents Sea across the four sections experience a more rapid change from pre-bloom to post-bloom conditions compared to if there had been no such gradient.

Our results showed an inverse relationship between phytoplankton timing and magnitude, both between sections and within sections between years. In the Barents Sea, nutrients are consumed by phytoplankton during the bloom period and replenished in winter by strong vertical mixing caused by heat losses and strong winds (Oziel et al. 2017). According to the critical-depth model (Sverdrup 1953), the spring bloom is mainly triggered by a combination of stratification of the water column and adequate light conditions. However, field investigations in both the Barents Sea and the Bering Sea indicated that spring blooms can develop prior to stratification (Eilertsen et al. 1993, Eslinger & Iverson 2001, Stabeno et al. 2010). We hypothesize that the negative correlation between bloom timing and magnitude is caused by nutrients consumption prior to the bloom. Specifically, when a bloom is early, no nutrients depletion occurs prior to the bloom, whereas when a bloom is late, some of the nutrients are consumed prior to the main bloom and thereby result in a lower magnitude.

There are pronounced seasonal patterns for both small- and medium-sized zooplankton: we found that biomass of both groups increase from March to July and decline thereafter. However, seasonal variation in biomass of large-sized zooplankton is inconspicuous. These differences might be due to the different life spans of the size groups. Large-sized zooplankton often have multi-year life-cycles, with lower potential for seasonal fluctuations in biomass than species with one or more generations per year. For example, two krill species that contribute to the large size group, *Thysanoessa longicaudata* and *Thysanoessa inermis*, have life spans of up to 2 years and 3-4 year, respectively (Dalpadado & Skjoldal 1996). On the other hand, two

generations of *Oithona similis* (small size) within one year was observed in the Kola Bay (Dvoretsky & Dvoretsky 2009), and *C. finmarchicus* (medium size) has mainly a one-year life cycle in the southwestern Barents Sea (Melle et al. 2014).

Biomass of both small- and medium-sized zooplankton varied from year to year during our study period, while the large-sized group showed first a decrease (from 1998 to 2015) and then increase (from 2015 to 2019). These trends are largely in line with a previous study (Stige et al. 2014), and adds to that study by showing trends in recent years, e.g. revealing the increase of large-sized zooplankton biomass. Stige et al. (2014) found that the interannual trends for small and medium-sized zooplankton correlated negatively with a jellyfish index, indicating that jellyfish predation might contribute to the variation. The interannual trend of large-sized zooplankton biomass correlated with a strong temperature increase from spring to summer, an indication of large inflow of warm Atlantic water from the Norwegian Sea (Stige et al. 2014). The biomass of krill, a main large-sized zooplankton group in our study region, is strongly associated with transport of *Meganyctiphanes norvegica* and *T. inermis* with Atlantic water into the Barents Sea (Orlova et al. 2013, Orlova et al. 2015, Eriksen et al. 2017). Note, however, that our finding of highest biomass of large-sized zooplankton at low temperatures seems to rather suggest an influence of more arctic species such as the amphipod *Themisto libellula* and the copepod *C. hyperboreus* (Dalpadado et al. 2012).

4.3 Association between Chl-*a* peak time and zooplankton biomass

Bloom timing can affect the energy transfer to higher trophic levels and carbon recycling by influencing the temporal match with zooplankton consumption (Cushing 1990, Winder & Schindler 2004). In Arctic and subarctic pelagic ecosystems, the timing of the bloom plays an

important role in influencing the life strategies of herbivorous mesozooplankton species (Falk-Petersen et al. 2009).

C. finmarchicus, the dominant mesozooplankton species in the southwestern Barents Sea (Aarflot et al. 2018), relies on phytoplankton as food to underpin egg production and new zooplankton generation growth (Melle & Skjoldal 1998, Hirche & Kosobokova 2003). The species overwinters at depth in the Norwegian Sea, ascend and spawn in early spring and are transported into the Barents Sea with the Atlantic Current (Skjoldal et al. 1992, Torgersen & Huse 2005). Local production and overwintering of *C. finmarchicus* in the Barents Sea are likely also non-negligible (Dalpadado et al. 2012, Kvile et al. 2017). Subsequently, individuals of the new generation develop to copepodite stage CIV or CV and then descend to diapause, or reach the adult stage CVI and reproduce within the same year, resulting in a second generation (Melle et al. 2004).

C. finmarchicus, as a temperate species, has smaller lipid reserves than more arctic congeners and is highly dependent on food to finish gonad maturation and initiate spawning (Niehoff et al. 2002, Madsen et al. 2008). Although the spawning of a minority of *C. finmarchicus* may start prior to the onset of the phytoplankton spring bloom, the main spawning period is triggered by the phytoplankton spring bloom (Hirche 1996, Melle & Skjoldal 1998, Niehoff et al. 1999). Therefore, an early phytoplankton bloom (e.g. late April or early May) may match better with the early spawning and developmental progress of *C. finmarchicus.* The new generation may subsequently develop earlier and reach the stages in the medium-sized zooplankton class (copepodite stage CIII and above) earlier. Our results confirmed that the biomass of the medium size class, dominated by *C. finmarchicus* in these developmental stages, was highest when the phytoplankton bloom was early. In contrast, a late phytoplankton bloom

(e.g. after May) may result in a relative late spawning of *C. finmarchicus* and thereby lower medium-sized zooplankton biomass during the main sampling season (August and September). In addition, a late bloom could lead to mismatch in timing of the phytoplankton bloom and timing of *C. finmarchicus* emergence from overwintering, resulting in lower egg production and success of the new generation.

As temperature effects were accounted for in the statistical analysis, we do not think that the associations between Chl-*a* peak timing and -magnitude and zooplankton biomass were caused by temperature jointly influencing phytoplankton and zooplankton dynamics. Nonetheless, we note that high temperature in the region has been associated with low late-summer Chl-*a* concentrations (Dong et al. 2020) and with early timing and high abundance of *C. finmarchicus* copepodites (Kvile et al. 2014). Our finding of highest June biomass of medium-sized zooplankton at high temperatures is consistent with the latter study. A mechanism that may contribute to such an association is that egg production and growth rate of *C. finmarchicus* scale positively with temperatures in the range 0-10 °C (Campbell et al. 2001, Kjellerup et al. 2012, Pasternak et al. 2013).

Our results indicate that the biomass of small-sized zooplankton was highest in years when the peak of the phytoplankton bloom occurred in mid-May or later (Fig. 6A). We propose the following hypotheses: First, as addressed above, if the spring bloom starts early, the spawning of *C. finmarchicus* is early. Their offspring develop early and have already transitioned from the small size group into the medium size group by the main time of sampling in August and September, thus resulting in low small-sized biomass in years with an early bloom. On the other hand, a late spring bloom results in late main spawning of *C. finmarchicus* and in a lagging development of the new generation. Consequently, by the main time of sampling in August and

September, they still stay in the small size group because of late and slow development. Second, small mesozooplankton species may be better able to take advantage of a late bloom than what medium-sized mesozooplankton are. Small species (e.g. *Oithona* spp.) start to dominate the surface layer in summer, and may therefore take advantage of a late bloom. Svensen et al. (2011) suggested that a tight connection with the microbial part of the food web plays a great role for the success of small copepods like *Oithona* spp. in autumn. Generally, there is a significant shift in species composition between the peaks of the diatom bloom in May and the coccolithophore bloom in August. Iversen and Seuthe (2011) reported that after the spring bloom period, small phytoplankton cells (<10 µm) generally dominate the phytoplankton community in the arctic ecosystem around Kongsfjorden. *Calanus* spp. mainly take advantage of the spring bloom which is dominated by large diatoms cells (>10 µm) for reproduction, while *Oithona* spp., which has more flexible reproductive strategy (Lischka & Hagen 2007), could make use of the microbial food web in summer and autumn for feeding and reproduction after the spring bloom.

4.4 Association between Chl-*a* peak magnitude and zooplankton biomass

In addition to the timing of the phytoplankton bloom, the peak magnitude and the duration of the bloom are also likely to play important roles for zooplankton development. Our results indicate a negative association between biomass of all three size fractions and high Chl-*a* peak magnitude (i.e. >5 mg m^{-3}). On one hand, these results seem to suggest that high phytoplankton bloom magnitude is detrimental to the zooplankton biomass in the southern Barents Sea. Model predictions have shown that if copepods are food saturated during the spring bloom, a further increase in magnitude beyond the saturation concentration will not promote copepod egg production, whereas a longer bloom duration will (Møller et al. 2016). In other words, a longer but relative weak bloom is more beneficial for *C. finmarchicus* than a short and

intense bloom. As mentioned previously (Section 4.2), the replenishment of nutrients to upper water layers occurs during winter and stops when the stratification is established. The amount of nutrients is generally highest at the beginning of the spring bloom. An intense bloom with high magnitude and consequently fast nutrients depletion will result in a short bloom duration and further hamper the zooplankton biomass increase. Therefore, the low biomass of zooplankton under high Chl-*a* peak magnitude conditions (i.e. >5 mg m^{-3}) might reflect an indirect influence of bloom magnitude on zooplankton biomass through bloom duration. Another possibility is that these results reflect a top-down control of phytoplankton magnitude by zooplankton predation (Strom et al. 2007). In this case, low biomass of zooplankton represents low feeding pressure on phytoplankton, which allowed the development of a high Chl-*a* peak.

Under low Chl-*a* peak magnitude conditions (i.e. <4 mg m^{-3}), biomass of small- and large-sized zooplankton increase with increasing Chl-*a* peak magnitude, while the biomass of the medium-sized group decreases. A possible interpretation is that at these Chl-*a* levels, higher bloom magnitude implies more food supply and thus higher population growth of zooplankton. We are uncertain why the medium-sized zooplankton appear to respond differently and have high biomass at low Chl-*a* peak magnitude. One possible explanation is a particularly strong top-down relationship between this dominant zooplankton size group and phytoplankton. In support of this interpretation, we note that *C. finmarchicus* CV and adults from the overwintering stock are ready to feed on the phytoplankton bloom when it starts and may therefore have stronger potential for top-down control than smaller and more short-lived species.

5. CONCLUSIONS

The Barents Sea has experienced a rapid warming trend over the last few decades (Sakshaug et al. 2009, Jakobsen & Ozhigin 2011) with expansion of relatively warm Atlantic water (Oziel et al. 2016, Neukermans et al. 2018). These trends are also projected to continue into the future (Sandø et al. 2014, Long & Perrie 2017, Onarheim & Årthun 2017). These changes in ocean climate could have great influence on the timing and magnitude of phytoplankton blooms and further affect the coupling with higher trophic levels. Our results indicate that an early spring bloom (e.g. late April or early May) increases medium-sized zooplankton biomass but decreases the biomass of the small-sized group. In this part of the Barents Sea, medium-sized zooplankton such as *C. finmarchicus* are key prey for commercially and ecologically important fishes including capelin (*Mallotus villosus*) and juvenile stages of cod (*Gadus morhua*) and haddock (*Melanogrammus aeglefinus*). Mesocosm experiments suggest that increasing temperature in high-latitude regions can lead to earlier stratification and onset of spring blooms (Lewandowska & Sommer 2010), although observations from the open waters of the Barents Sea do not show any clear trend of bloom timing in recent decades (Dalpadado et al. 2020 and Fig. 3). Our results imply that possible earlier bloom timing with future warming would benefit planktivorous fishes that feed on medium-sized zooplankton.

Our results further suggest that increased bloom magnitude above 5 mg m^{-3} reduces zooplankton biomass. Possibly, an intense bloom with high magnitude consumes nutrients in the stratified water layer rapidly and results in a short bloom duration, which restrains the zooplankton population growth. Alternatively, high bloom magnitude can be an indication of low feeding pressure from zooplankton and a foreboding of low zooplankton biomass also in the

months to come. In sum, our study underlines the importance of investigating how future warming may impact not only the timing but also the magnitude and duration of spring blooms.

6. ACKNOWLEDGEMENTS

K.D. was supported by the China Scholarship Council. K.Ø.K was funded by VISTA – a basic research program in collaboration between The Norwegian Academy of Science and Letters, and Equinor. L.C.S. was supported by Research Council of Norway project 280468 ("Drivers and effects of spatial shifts in early life stages of marine fish – SpaceShift"). We thank the Institute of Marine Research and the Norwegian Data Centre for providing zooplankton data.

7. REFERENCES

Aarflot JM, Skjoldal HR, Dalpadado P, Skern-Mauritzen M (2018) Contribution of *Calanus* species to the mesozooplankton biomass in the Barents Sea. ICES J Mar Sci 75:2342-2354

Asplin L, Budgell P, Ingvaldsen R, Lien V, Loeng H, Skagseth Ø (2006) Comparison of modelled and measured fluxes at the western Barents Slope. Deliverable D2 6, WP 2, ASOF

Behrenfeld MJ, Boss ES (2014) Resurrecting the ecological underpinnings of ocean plankton blooms. Annu Rev Mar Sci 6:167-194

Blanchard JL, Heneghan RF, Everett JD, Trebilco R, Richardson AJ (2017) From bacteria to whales: using functional size spectra to model marine ecosystems. Trends Ecol Evol 32:174-186

Campbell RG, Wagner MM, Teegarden GJ, Boudreau CA, Durbin EG (2001) Growth and development rates of the copepod *Calanus finmarchicus* reared in the laboratory. Mar Ecol Prog Ser 221:161-183

Cloern JE, Foster S, Kleckner A (2014) Phytoplankton primary production in the world's estuarine-coastal ecosystems. Biogeosciences 11:2477

Cushing D (1990) Plankton production and year-class strength in fish populations: an update of the match/mismatch hypothesis. Adv Mar Biol, Book 26. Elsevier

Dalpadado P, Arrigo KR, van Dijken GL, Skjoldal HR, Bagøien E, Dolgov AV, Prokopchuk IP, Sperfeld E (2020) Climate effects on temporal and spatial

dynamics of phytoplankton and zooplankton in the Barents Sea. Prog Oceanogr 185:pp. 102320
Dalpadado P, Ingvaldsen RB, Stige LC, Bogstad B, Knutsen T, Ottersen G, Ellertsen B (2012) Climate effects on Barents Sea ecosystem dynamics. ICES J Mar Sci 69:1303-1316
Dalpadado P, Skjoldal HR (1996) Abundance, maturity and growth of the krill species *Thysanoessa inermis* and *T. longicaudata* in the Barents Sea. Mar Ecol Prog Ser 144:175-183
Dong K, Kvile Ø, Stenseth NC, Stige LC (2020) Associations among temperature, sea ice and phytoplankton bloom dynamics in the Barents Sea. Mar Ecol Prog Ser 635:25-36
Dvoretsky V, Dvoretsky A (2009) Life cycle of *Oithona similis* (Copepoda: Cyclopoida) in Kola Bay (Barents Sea). Mar Biol 156:1433-1446
Edvardsen A, Slagstad D, Tande K, Jaccard P (2003) Assessing zooplankton advection in the Barents Sea using underway measurements and modelling. Fish Oceanogr 12:61-74
Eilertsen H-C, Hansen G, Svendsen H, Hegseth E (1993) Onset of the spring phytoplankton bloom in the Barents Sea: influence of changing light regime and other environmental factors ctors. In: Eilertsen HC (ed) Underwater light measurements. SPIE Proc 2048: 20-32
Eriksen E, Skjoldal HR, Gjøsæter H, Primicerio R (2017) Spatial and temporal changes in the Barents Sea pelagic compartment during the recent warming. Prog Oceanogr 151:206-226
Ersdal G (2001) An overview of ocean currents with emphasis on currents on the Norwegian continental shelf. NPD Preliminary Report:1-40
Eslinger DL, Iverson RL (2001) The effects of convective and wind-driven mixing on spring phytoplankton dynamics in the southeastern Bering Sea middle shelf domain. Cont Shelf Res 21:627-650
Falk-Petersen S, Hop H, Budgell WP, Hegseth EN, Korsnes R, Løyning TB, Ørbæk JB, Kawamura T, Shirasawa K (2000) Physical and ecological processes in the marginal ice zone of the northern Barents Sea during the summer melt period. J Mar Syst 27:131-159
Falk-Petersen S, Mayzaud P, Kattner G, Sargent JR (2009) Lipids and life strategy of Arctic *Calanus*. Mar Biol Res 5:18-39
Falk-Petersen S, Pavlov V, Timofeev S, Sargent JR (2007) Climate variability and possible effects on arctic food chains: the role of *Calanus*. In: Ørbæk JB, Tombre T, Kallenborn R, Hegseth E, Falk-Petersen S, Hoel AH (eds) Arctic

alpine ecosystems and people in a changing environment. Springer-Verlag. Berlin, p 147–166.
Friedland KD, Leaf RT, Kane J, Tommasi D, Asch RG, Rebuck N, Ji R, Large SI, Stock C, Saba VS (2015) Spring bloom dynamics and zooplankton biomass response on the US Northeast Continental Shelf. Cont Shelf Res 102:47-61
Friedland KD, Mouw CB, Asch RG, Ferreira ASA, Henson S, Hyde KJ, Morse RE, Thomas AC, Brady DC (2018) Phenology and time series trends of the dominant seasonal phytoplankton bloom across global scales. Glob Ecol Biogeogr 27:551-569
Gjøsæter H, Dalpadado P, Hassel A (2002) Growth of Barents Sea capelin (*Mallotus villosus*) in relation to zooplankton abundance. ICES J Mar Sci 59:959-967
Griffiths JR, Kadin M, Nascimento FJ, Tamelander T, Törnroos A, Bonaglia S, Bonsdorff E, Brüchert V, Gårdmark A, Järnström M (2017) The importance of benthic–pelagic coupling for marine ecosystem functioning in a changing world. Glob Change Biol 23:2179-2196
Guinder V, Molinero JC (2013) Climate change effects on marine phytoplankton. In:Arias AH, Menendez MC (eds) Marine ecology in a changing world. CRC Press, Boca Raton, FL, p 68−90.
Hastie T, Tibshirani R (1993) Varying-coefficient models. J R Stat Soc Series B Stat Methodol 55:757-779
Hastie TJ, Tibshirani RJ (1990) Generalized additive models. Chapman & Hall, London
Hirche H-J (1996) Diapause in the marine copepod, *Calanus finmarchicus*—a review. Ophelia 44:129-143
Hirche H-J, Kosobokova K (2003) Early reproduction and development of dominant calanoid copepods in the sea ice zone of the Barents Sea—need for a change of paradigms? Mar Biol 143:769-781
Hooff RC, Peterson WT (2006) Copepod biodiversity as an indicator of changes in ocean and climate conditions of the northern California current ecosystem. Limnol Oceanogr 51:2607-2620
Ingvaldsen RB, Asplin L, Loeng H (2004) The seasonal cycle in the Atlantic transport to the Barents Sea during the years 1997–2001. Cont Shelf Res 24:1015-1032
Iversen KR, Seuthe L (2011) Seasonal microbial processes in a high-latitude fjord (Kongsfjorden, Svalbard): I. Heterotrophic bacteria, picoplankton and nanoflagellates. Polar Biol 34:731-749

Jakobsen T, Ozhigin VK (2011) Introduction to the Barents Sea. In: Jakobsen T, Ozhigin VK (eds) The Barents Sea: ecosystem, resources, management: half a century of Russian-Norwegian cooperation. Tapir academic press Trondheim

Kahru M, Lee Z, Mitchell BG, Nevison CD (2016) Effects of sea ice cover on satellite-detected primary production in the Arctic Ocean. Biol Lett 12:20160223

Kjellerup S, Dünweber M, Swalethorp R, Nielsen TG, Møller EF, Markager S, Hansen BW (2012) Effects of a future warmer ocean on the coexisting copepods Calanus finmarchicus and C. glacialis in Disko Bay, western Greenland. Mar Ecol Prog Ser 447:87-108

Kvile KØ, Dalpadado P, Orlova E, Stenseth NC, Stige LC (2014) Temperature effects on Calanus finmarchicus vary in space, time and between developmental stages. Mar Ecol Prog Ser 517:85-104

Kvile KØ, Fiksen Ø, Prokopchuk I, Opdal AF (2017) Coupling survey data with drift model results suggests that local spawning is important for *Calanus finmarchicus* production in the Barents Sea. J Mar Syst 165:69-76

Kvile KØ, Langangen Ø, Prokopchuk I, Stenseth NC, Stige LC (2016) Disentangling the mechanisms behind climate effects on zooplankton. Proc Natl Acad Sci USA 113:1841-1846

Leu E, Søreide J, Hessen D, Falk-Petersen S, Berge J (2011) Consequences of changing sea-ice cover for primary and secondary producers in the European Arctic shelf seas: timing, quantity, and quality. Prog Oceanogr 90:18-32

Lewandowska A, Sommer U (2010) Climate change and the spring bloom: a mesocosm study on the influence of light and temperature on phytoplankton and mesozooplankton. Mar Ecol Prog Ser 405:101-111

Lischka S, Hagen W (2007) Seasonal lipid dynamics of the copepods *Pseudocalanus minutus* (Calanoida) and *Oithona similis* (Cyclopoida) in the Arctic Kongsfjorden (Svalbard). Mar Biol 150:443-454

Loeng H (1991) Features of the physical oceanographic conditions of the Barents Sea. Polar Res 10:5-18

Long Z, Perrie W (2017) Changes in ocean temperature in the Barents Sea in the twenty-first century. J Clim 30:5901-5921

Madsen SJ, Nielsen TG, Tervo OM, Söderkvist J (2008) Importance of feeding for egg production in Calanus finmarchicus and C. glacialis during the Arctic spring. Mar Ecol Prog Ser 353:177-190

Maritorena S, d'Andon OHF, Mangin A, Siegel DA (2010) Merged satellite ocean color data products using a bio-optical model: Characteristics, benefits and issues. Remote Sens Environ 114:1791-1804

Melle W, Ellertsen B, Skjoldal H (2004) Zooplankton: the link to higher trophic levels. In: Skjoldal HR (ed) The Norwegian Sea ecosystem. Tapir Academic Press, Trondheim, p 137–202.

Melle W, Runge J, Head E, Plourde S, Castellani C, Licandro P, Pierson J, Jonasdottir S, Johnson C, Broms C (2014) The North Atlantic Ocean as habitat for Calanus *finmarchicus*: Environmental factors and life history traits. Prog Oceanogr 129:244-284

Melle W, Skjoldal HR (1998) Reproduction and development of *Calanus finmarchicus*, *C. glacialis* and *C. hyperboreus* in the Barents Sea. Mar Ecol Prog Ser 169:211-228

Møller EF, Bohr M, Kjellerup S, Maar M, Møhl M, Swalethorp R, Nielsen TG (2016) *Calanus finmarchicus* egg production at its northern border. J Plankton Res 38:1206-1214

Møller EF, Nielsen TG (2020) Borealization of Arctic zooplankton—smaller and less fat zooplankton species in Disko Bay, Western Greenland. Limnol Oceanogr 65:1175-1188

Mosby H (1968) Surrounding seas. Geography of Norden. JW Cappelens Forlag Oslo, Norway

Neukermans G, Oziel L, Babin M (2018) Increased intrusion of warming Atlantic water leads to rapid expansion of temperate phytoplankton in the Arctic. Glob Change Biol 24:2545-2553

Niehoff B, Klenke U, Hirche H-J, Irigoien X, Head R, Harris R (1999) A high frequency time series at Weathership M, Norwegian Sea, during the 1997 spring bloom: the reproductive biology of *Calanus finmarchicus*. Mar Ecol Prog Ser 176:81-92

Niehoff B, Madsen S, Hansen B, Nielsen T (2002) Reproductive cycles of three dominant Calanus species in Disko Bay, West Greenland. Mar Biol 140:567-576

Nixon SW, Fulweiler RW, Buckley BA, Granger SL, Nowicki BL, Henry KM (2009) The impact of changing climate on phenology, productivity, and benthic–pelagic coupling in Narragansett Bay. Estuar Coast Shelf Sci 82:1-18

Ohashi R, Yamaguchi A, Matsuno K, Saito R, Yamada N, Iijima A, Shiga N, Imai I (2013) Interannual changes in the zooplankton community structure on the

southeastern Bering Sea shelf during summers of 1994–2009. Deep Sea Res II 94:44-56
Onarheim IH, Årthun M (2017) Toward an ice-free Barents Sea. Geophys Res Lett 44:8387-8395
Orlova EL, Dolgov AV, Renaud PE, Boitsov VD, Prokopchuk IP, Zashihina MV (2013) Structure of the macroplankton–pelagic fish–cod trophic complex in a warmer Barents Sea. Mar Biol Res 9:851-866
Orlova EL, Dolgov AV, Renaud PE, Greenacre M, Halsband C, Ivshin VA (2015) Climatic and ecological drivers of euphausiid community structure vary spatially in the Barents Sea: relationships from a long time series (1952–2009). Front Mar Sci 1:74
Oziel L, Neukermans G, Ardyna M, Lancelot C, Tison JL, Wassmann P, Sirven J, Ruiz-Pino D, Gascard JC (2017) Role for Atlantic inflows and sea ice loss on shifting phytoplankton blooms in the Barents Sea. J Geophys Res, C, Oceans 122:5121-5139
Oziel L, Sirven J, Gascard J-C (2016) The Barents Sea frontal zones and water masses variability (1980–2011). Ocean Sci 12:169-184
Pasternak A, Arashkevich E, Grothe U, Nikishina A, Solovyev K (2013) Different effects of increased water temperature on egg production of Calanus finmarchicus and C. glacialis. Oceanology (Mosc) 53:547-553
Pyper BJ, Peterman RM (1998) Comparison of methods to account for autocorrelation in correlation analyses of fish data. Can J Fish Aquat Sci 55:2127-2140
Quenouille MH (1952) Associated measurements. Butterworth, London
R Core Team (2018) R: a language and environment for statistical computing. R Foundation for Statistical Computing, Vienna.
Reigstad M, Wassmann P, Riser CW, Øygarden S, Rey F (2002) Variations in hydrography, nutrients and chlorophyll a in the marginal ice-zone and the central Barents Sea. J Mar Syst 38:9-29
Reygondeau G, Beaugrand G (2011) Future climate-driven shifts in distribution of *Calanus finmarchicus*. Glob Change Biol 17:756-766
Reynolds RW, Smith TM, Liu C, Chelton DB, Casey KS, Schlax MG (2007) Daily high-resolution-blended analyses for sea surface temperature. J Clim 20:5473-5496
Rice E, Dam HG, Stewart G (2015) Impact of climate change on estuarine zooplankton: surface water warming in Long Island Sound is associated

with changes in copepod size and community structure. Estuar Coasts 38:13-23
Richardson AJ (2008) In hot water: zooplankton and climate change. ICES J Mar Sci 65:279-295
Sakshaug E, Johnsen GH, Kovacs KM (2009) Ecosystem Barents Sea. Tapir Academic Press, Trondheim. Tapir Academic Press
Sandø AB, Melsom A, Budgell WP (2014) Downscaling IPCC control run and future scenario with focus on the Barents Sea. Ocean Dyn 64:927-949
Signorini SR, McClain CR (2009) Environmental factors controlling the Barents Sea spring-summer phytoplankton blooms. Geophys Res Lett 36
Skjoldal HR, Gjøsæter H, Loeng H The Barents Sea ecosystem in the 1980s. ocean climate, plankton, and capelin growth. ICES Mar Sci Symp 195:278-290
Sommer U, Adrian R, De Senerpont Domis L, Elser JJ, Gaedke U, Ibelings B, Jeppesen E, Lürling M, Molinero JC, Mooij WM (2012) Beyond the Plankton Ecology Group (PEG) model: mechanisms driving plankton succession. Annu Rev Ecol Evol Syst 43:429-448
Sommer U, Lengfellner K (2008) Climate change and the timing, magnitude, and composition of the phytoplankton spring bloom. Glob Change Biol 14:1199-1208
Søreide JE, Leu EV, Berge J, Graeve M, Falk-Petersen S (2010) Timing of blooms, algal food quality and *Calanus glacialis* reproduction and growth in a changing Arctic. Glob Change Biol 16:3154-3163
Stabeno P, Napp J, Mordy C, Whitledge T (2010) Factors influencing physical structure and lower trophic levels of the eastern Bering Sea shelf in 2005: Sea ice, tides and winds. Prog Oceanogr 85:180-196
Stige LC, Dalpadado P, Orlova E, Boulay A-C, Durant JM, Ottersen G, Stenseth NC (2014) Spatiotemporal statistical analyses reveal predator-driven zooplankton fluctuations in the Barents Sea. Prog Oceanogr 120:243-253
Strom SL, Macri EL, Olson MB (2007) Microzooplankton grazing in the coastal Gulf of Alaska: Variations in top-down control of phytoplankton. Limnol Oceanogr 52:1480-1494
Svensen C, Seuthe L, Vasilyeva Y, Pasternak A, Hansen E (2011) Zooplankton distribution across Fram Strait in autumn: Are small copepods and protozooplankton important? Prog Oceanogr 91:534-544
Sverdrup H (1953) On conditions for the vernal blooming of phytoplankton. J Cons Int Explor Mer 18:287-295

Torgersen T, Huse G (2005) Variability in retention of *Calanus finmarchicus* in the Nordic Seas. ICES J Mar Sci 62:1301-1309

Ueyama R, Monger BC (2005) Wind-induced modulation of seasonal phytoplankton blooms in the North Atlantic derived from satellite observations. Limnol Oceanogr 50:1820-1829

Wassmann P (2011) Arctic marine ecosystems in an era of rapid climate change. Prog Oceanogr 90:1-17

Wassmann P, Slagstad D, Riser CW, Reigstad M (2006) Modelling the ecosystem dynamics of the Barents Sea including the marginal ice zone: II. Carbon flux and interannual variability. J Mar Syst 59:1-24

Winder M, Schindler DE (2004) Climate change uncouples trophic interactions in an aquatic ecosystem. Ecology 85:2100-2106

Winder M, Sommer U (2012) Phytoplankton response to a changing climate. Hydrobiologia 698:5-16

Table 1. Performance of models describing associations between different zooplankton size groups at section D and Chl-*a* peak timing and magnitude at sections A-D (Eq. 6).

			Small-sized zooplankton			**Medium-sized zooplankton**			**Large-sized zooplankton**
Sections	R^2	GCV	P values *ptime*/*pmag*	R^2	GCV	P values *ptime*/*pmag*	R^2	GCV	P values *ptime*/*pmag*
A	0.467	0.173	/***	0.265	0.213	/	**0.168**	**0.186**	**/****
B	0.455	0.176	/**	0.272	0.211	·/·	0.147	0.191	/
C	0.457	0.176	/**	**0.300**	**0.202**	***/***	0.144	0.191	/
D	**0.477**	**0.170**	***/*** **	0.293	0.205	**/***	0.148	0.190	/

Note: R^2: proportion of deviance explained; GCV: generalized cross-validation criterion. Models with lower GCV has more predictive power. Bold numbers indicate the best performance of tested models. P-values refer to effects of *ptime* and *pmag* in Eq. 6.

Significance codes: "***" refers to $p < 0.001$; "**" $p < 0.01$; "*" $p < 0.05$; "·" $p < 0.1$; blank refers to $p > 0.1$.

Table 2. Model selection results for different zooplankton size groups from section D and explanatory Chl-*a* indices from sections identified in Table 1.

	Small-sized zooplankton		**Medium-sized zooplankton**		**Large-sized zooplankton**	
Models	R^2	CV	R^2	CV	R^2	CV
(1) f(*doy*) + g(*logdepth*)	0.399	0.447	0.253	0.460	0.074	0.453
(2) f(*doy*) + g(*logdepth*) + h(*year*)	0.441	-	0.282	-	0.154	-
(3) F(*doy,SST*) + g(*logdepth*)	0.446	0.422	0.261	0.456	0.144	0.446
(4) F(*doy,SST*) + g(*logdepth*) + k(*ptime*)	0.453	0.422	0.277	0.457	0.152	0.444
(5) F(*doy,SST*) + g(*logdepth*) + l(*pmag*)	0.469	0.420	0.269	0.459	0.166	**0.437**
(6) F(*doy,SST*) + g(*logdepth*) + k(*ptime*) + l(*pmag*)	0.477	**0.4180**	0.300	**0.448**	0.168	0.438
(7) F(*doy,SST*) + g(*logdepth*) + K(*ptime, doy*) + l(*pmag*)	0.470	0.4183	0.299	0.453	0.171	0.438
(8) F(*doy,SST*)+ g(*logdepth*) + k(*ptime*) + L(*pmag, doy*)	0.463	0.432	0.301	0.449	0.160	0.443

Note: R^2: proportion of deviance explained; CV: cross-validation criterion (leave one year out root-mean-squared prediction error). Models with lower CV values have higher out-of-sample predictive power. Bold numbers indicate the models with lowest CV. It was not meaningful to calculate the CV of Model 2 because it included year (shown by "-").

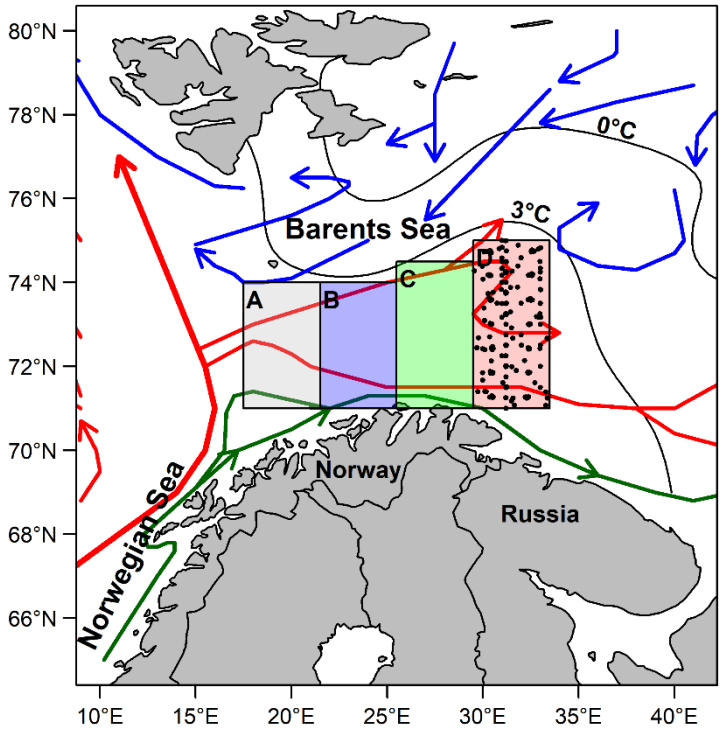

Figure 1. Study area. A-D represent the four research sections considered. The arrows show the prevailing surface currents: blue, Arctic Current; red, Atlantic Current; green, Norwegian Coastal Current. Black points represent zooplankton data. Black contour lines show the long-term mean 0 °C and 3 °C temperature isolines in August–October in the Barents Sea.

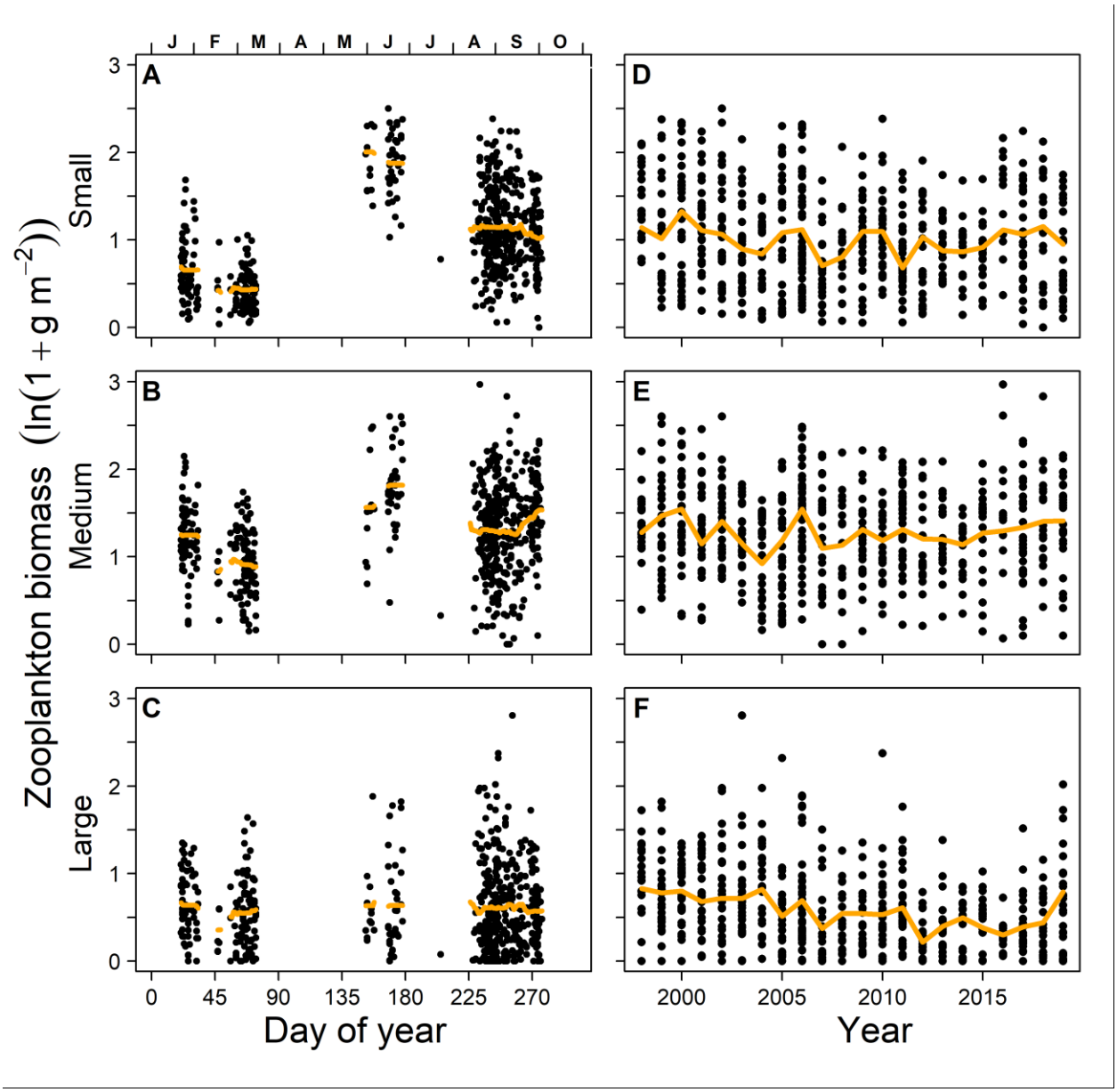

Figure 2. Zooplankton data. Black symbols: biomass of zooplankton in section D plotted against day-of-year (panels A-C, with month indicated above panel A) or year (panels D-F). Each row represents one zooplankton size fraction (A and D: Small, 0.18–1 mm, B and E: Medium, 1–2 mm, C and F: Large, >2 mm). Orange lines in left panels show running mean (± 10 days) of ln-scaled zooplankton biomass. Orange lines in right panels indicate the annual averages of ln-scaled zooplankton biomass.

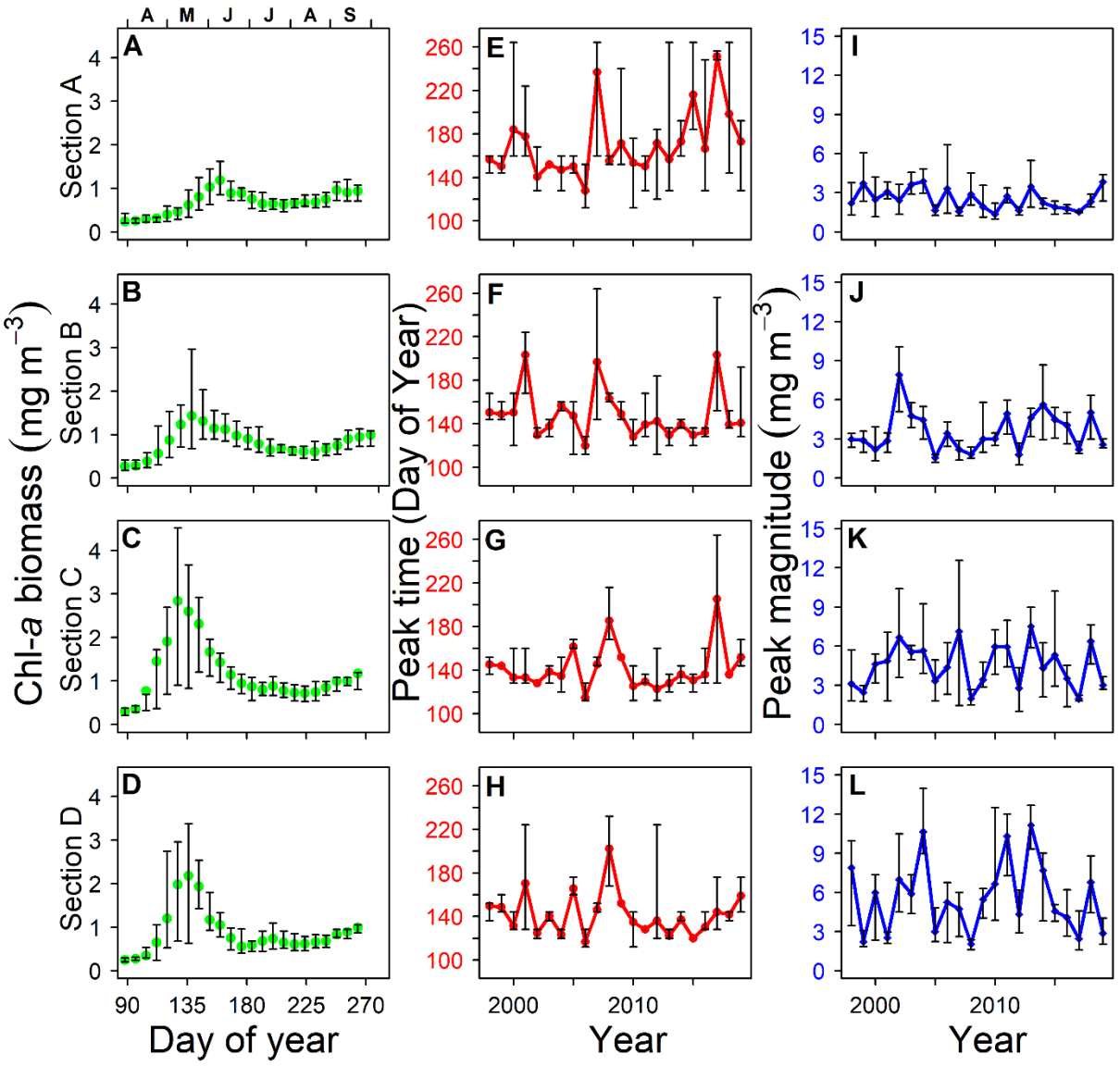

Figure 3. Chlorophyll *a* data. Left panels (A-D): green points with bars show median phytoplankton biomass with interquartile range for each 8-days period and section for all years. Middle panels (E-H) show interannual variability of averaged Chl-*a* peak time (red points and solid line) with interquartile range for each section. Right panels (I-L) show interannual variability of averaged Chl-*a* peak magnitude (blue points and solid line) with interquartile range for each section.

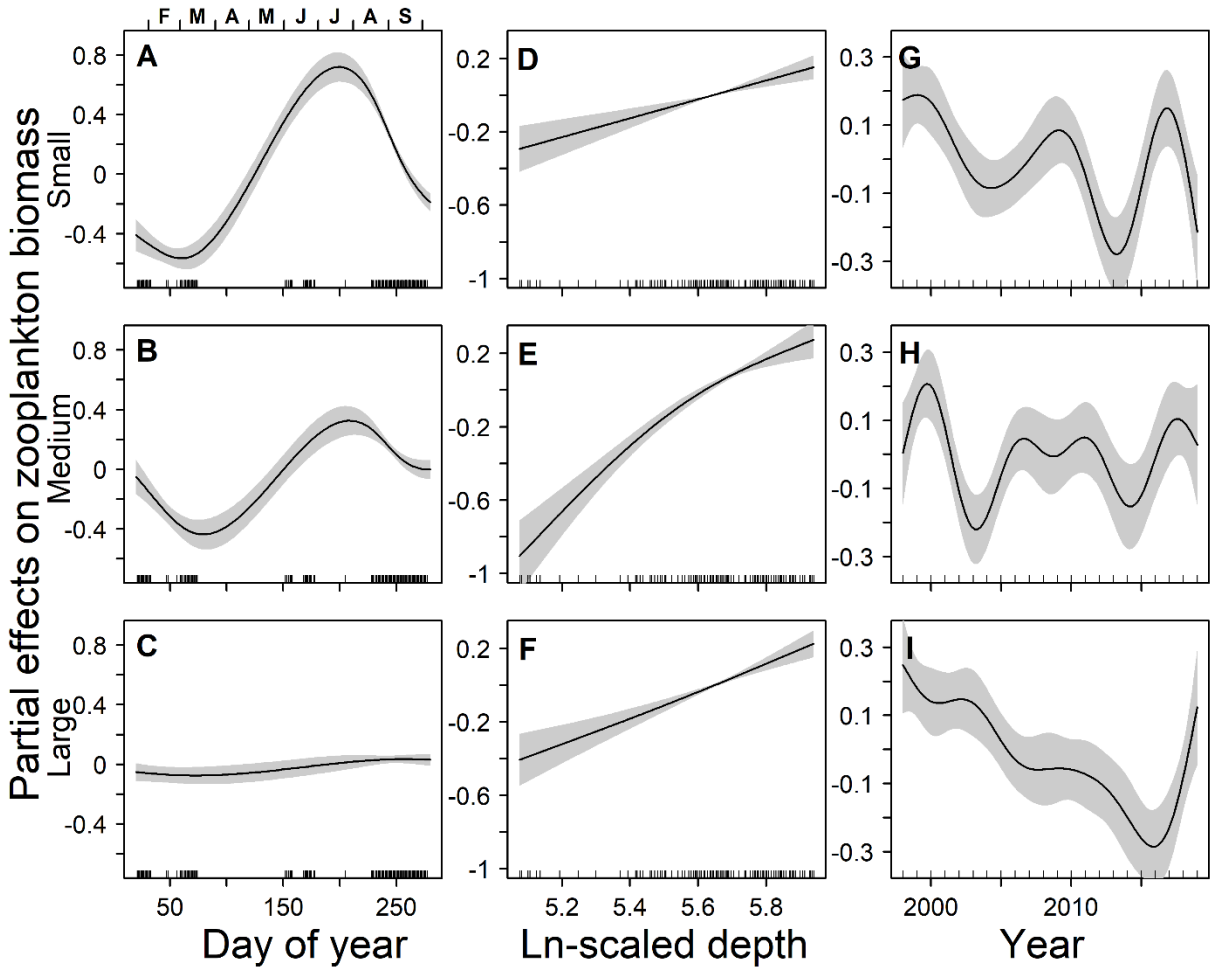

Figure 4. Season, sampling depth and year effects on zooplankton biomass [ln (1 + mg m^{-2})]. Lines and shaded areas show partial effects with 95% confidence intervals from generalized additive models (Eq. 2 in Table 2). Each row of panels shows the partial effects of day-of-year (A-C), log-scaled sampling depth (D-F), and biological year (G-I) on one zooplankton size group. The rugs along the x-axes indicate the location of observations.

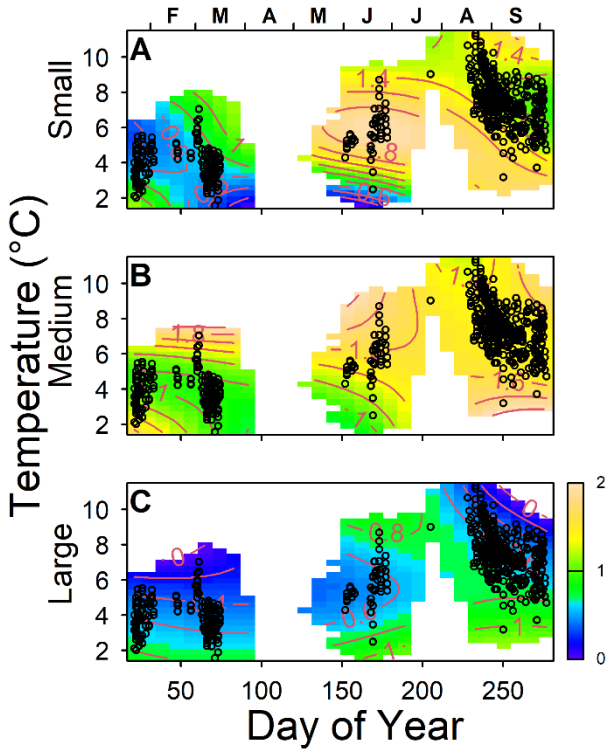

Figure 5. Predicted zooplankton biomass (mg m^{-2}) as function of day-of-year and SST. Each panel shows predictions from model 3 (Table 2) for one zooplankton size group. The color indicates the predicted biomass, with blue indicating low biomass and yellow high. White areas indicate combinations of day-of-year and temperature with insufficient data to make reliable predictions. Points show the locations of the data.

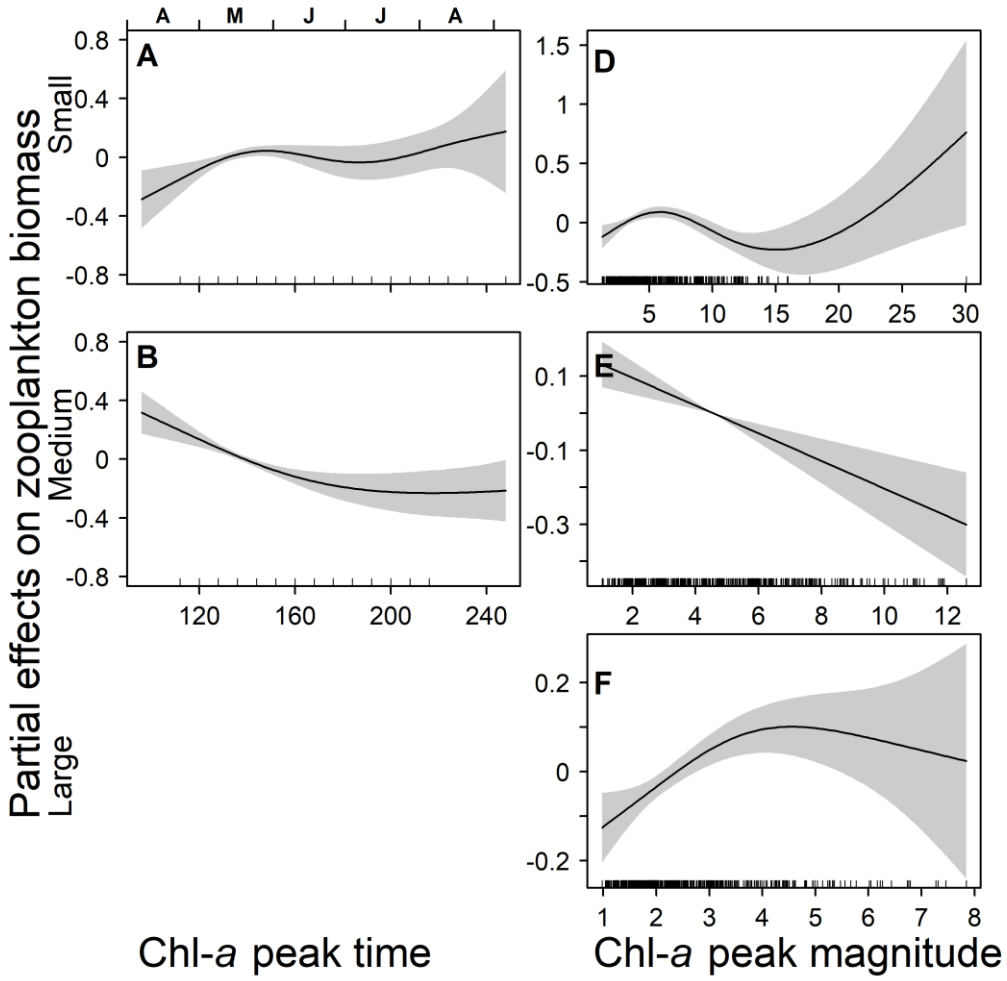

Figure 6. Effects of Chl-*a* peak time (*ptime*, day of year) and Chl-*a* peak magnitude (*pmag*, mg m^{-3}) on zooplankton biomass [ln (1 + mg m^{-2})]. The figure shows the partial effects of *ptime* (A and B) and *pmag* (D-F) in the best performing model for each zooplankton size-class. Lines and shaded areas show partial effects with 95% confidence intervals from generalized additive models (equations 5 and 6 in Table 2). Rugs along the x-axes indicate the location of data.

1